# Collective Motion of Humans in Mosh and Circle Pits at Heavy Metal Concerts

Jesse L. Silverberg,* Matthew Bierbaum, James P. Sethna, and Itai Cohen

*Department of Physics and Laboratory of Atomic and Solid State Physics, Cornell University, Ithaca, New York 14853, USA*

(Received 13 February 2013; published 29 May 2013)

Human collective behavior can vary from calm to panicked depending on social context. Using videos publicly available online, we study the highly energized collective motion of attendees at heavy metal concerts. We find these extreme social gatherings generate similarly extreme behaviors: a disordered gaslike state called a *mosh pit* and an ordered vortexlike state called a *circle pit*. Both phenomena are reproduced in flocking simulations demonstrating that human collective behavior is consistent with the predictions of simplified models.

DOI: 10.1103/PhysRevLett.110.228701 PACS numbers: 89.65.Ef, 47.32.−y, 87.15.Zg, 87.23.Cc

Human collective behaviors vary considerably with social context. For example, lane formation in pedestrian traffic [1], jamming during escape panic [2], and Mexican waves at sporting events [3] are emergent phenomena that have been observed in specific social settings. Here, we study large crowds ($10^2$–$10^5$ attendees) of people under the extreme conditions typically found at heavy metal concerts [4]. Often resulting in injuries [5], the collective mood is influenced by the combination of loud (130 dB [6]), fast (blast beats exceeding 300 beats per min) music, synchronized with bright flashing lights, and frequent intoxication [7]. This variety and magnitude of stimuli are atypical of more moderate settings and contribute to the collective behaviors studied here (Fig. 1).

Thousands of videos filmed by attendees at heavy metal concerts [8] highlight a collective phenomenon consisting of $10^1$–$10^2$ participants commonly referred to as a *mosh pit*. In traditional mosh pits, the participants (moshers) move randomly, colliding with one another in an undirected fashion (Fig. 2(a); see Supplemental Material for video metadata [9]). Mosh pits can form spontaneously or at the suggestion of the performing band, but in both cases, no micromanagement of individual actions is generally involved. Qualitatively, this phenomenon resembles the kinetics of gaseous particles, even though moshers are self-propelled agents that experience dissipative collisions and exist at a much higher density than most gaseous systems. To explore this analogy quantitatively, we watched over $10^2$ videos containing footage of mosh pits on YouTube.com, obtained six that were filmed from a suitably high position to provide a clear view of the crowd, corrected for perspective distortions [10] as well as camera instability, and used particle image velocimetry (PIV) analysis [11] to measure the two-dimensional (2D) velocity field on an interpolated grid [Fig. 2(b)].

Video data of mosh pits were used to calculate the velocity-velocity correlation function $c_{vv}$, where we noted an absence of the spatial oscillations typically found in liquidlike systems [Fig. 2(b) inset] [12]. Generally, $c_{vv}$ was well fit by a pure exponential, and for the video used in Fig. 2, the decay length was $0.39 \pm 0.03$ m, which is approximately human shoulder width. Taken together, these findings offer strong support for the analogy between mosh pits and gases. As a further check, we examined the 2D speed distribution. Previous observations of human pedestrian traffic and escape panic led us to expect a broad distribution not well described by simple analytic expressions [2,13]. However, the measured speed distribution in mosh pits was well fit by the 2D Maxwell-Boltzmann distribution, which is characterized by the probability distribution function $\mathrm{PDF}(v) = (2v/T)e^{-v^2/T}$ and temperature $T$ [Fig. 2(c) and inset] [14]. These observations present an interesting question: why does an inherently nonequilibrium system exhibit equilibrium characteristics?

Studies of collective motion in living and complex systems have found notable success within the framework of flocking simulations [15–23]. Thus, we use a Vicsek-like

FIG. 1 (color online). This photograph illustrates typical collective behavior found in a mosh pit at heavy metal concerts. Notice that some attendees are participating (foreground), while others are not (background). Image courtesy of Ulrike Biets.

 

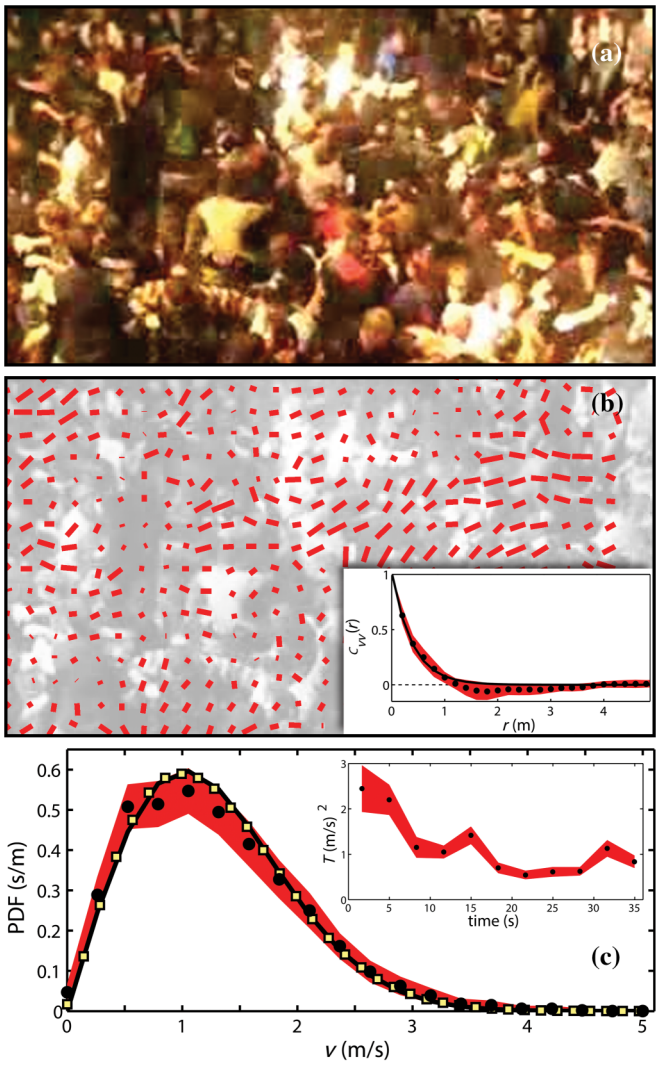


FIG. 2 (color online). (a) Single video frame illustrating a characteristic mosh pit [8]. (b) The same video image with overlaid velocity field. To facilitate comparisons with (a), this image is not corrected for perspective distortions. Inset shows the measured velocity-velocity correlation $c_{vv}$ (solid black circles) as a function of distance $r$, as well as the best fit to a pure exponential (black line, $R^2 = 0.97$). (c) The measured PDF for speed from the same video (solid black circles), the best fit to a 2D Maxwell-Boltzmann distribution (black line), and the speed distribution found in simulations (yellow squares). Inset shows the best-fit temperature as a function of time illustrating that an initially "hot" mosh pit "cools down." Error estimates are in red for all plots.

model [23] to simplify the complex behavioral dynamics of each human mosher to that of a simple soft-bodied particle we dub a mobile active simulated humanoid, or MASHer. Our model includes two species of MASHers to reflect the typical crowd at heavy metal concerts where we find both active and passive participants (Fig. 1, foreground and background, respectively) [24]. The first species, referred to as active MASHers repel during collisions, exhibit self-propulsion, experience flocking interactions, and are subject to random fluctuations due to environmental stimuli. These effects are modeled as forces on the $i$th MASHer by

$$\vec{F}_i^{\text{repulsion}} = \begin{cases} \epsilon\left(1 - \frac{r_{ij}}{2r_0}\right)^{3/2}\hat{r}_{ij} & r_{ij} < 2r_0 \\ 0 & \text{otherwise,} \end{cases} \quad (1)$$

$$\vec{F}_i^{\text{propulsion}} = \mu(v_0 - v_i)\hat{v}_i, \quad (2)$$

$$\vec{F}_i^{\text{flocking}} = \alpha \sum_{j=0}^{N_i} \vec{v}_j \Big/ \left| \sum_{j=1}^{N_i} \vec{v}_j \right|, \quad (3)$$

$$\vec{F}_i^{\text{noise}} = \vec{\eta}_i. \quad (4)$$

The Hertzian repulsion force [25] has a strength $\epsilon$, and is determined by the MASHer radius $r_0$, as well as the distance $r_{ij}$ and direction $\hat{r}_{ij}$ between MASHers $i$ and $j$. A variant of this expression with a 5/2 power law was tested and found to produce quantitatively similar results. The self-propulsion force has a strength $\mu$, is aligned with the MASHer heading $\hat{v}_i$, and is proportional to the difference between the current speed $v_i$ and the preferred speed $v_0$. The flocking force has a strength $\alpha$, and is in the direction found by vectorially averaging the headings of the $N_i$ MASHers within a distance $r_{\text{flock}} = 4r_0$ of MASHer $i$. Consistent with previous work [16,22,23], this distance was fixed in our model so that $r_0 < r_{\text{flock}} < L$, where $L$ is the system size. This choice minimizes the influence of finite-size effects on the flocking force [15]. Finally, the random force $\vec{\eta}_i$ is a vector whose components $\eta_{i,\lambda}$ are drawn from a Gaussian distribution with zero mean and standard deviation $\sigma$ defined by the correlation function $\langle \eta_{i,\lambda}(t)\eta_{i,\kappa}(t')\rangle = 2\mu\sigma^2\delta_{\lambda\kappa}\delta(t - t')$; the noise is spatially and temporally decorrelated. Based on observational evidence, the second species in our model, passive MASHers, prefer to remain stationary and are not subject to flocking interactions or random forces. Thus, in the appropriate units, we set $v_0 = 0$, $\alpha = 0$, and $\vec{\eta}_i = \vec{0}$ for passive MASHers. Active MASHers have $v_0 = 1$, while $\alpha$ and $\sigma$ were varied to explore the phase space of the model. The remaining parameters are the same for all MASHers, and were set to $\epsilon = 25$, $\mu = 1$, and $r_0 = 1$.

We simulated concerts with $N = 500$ MASHers at a packing fraction of $\rho = 0.94$. Thirty percent of the population was active, while the remaining was passive. Periodic boundary conditions were employed to avoid edge effects, and numerical integration of $\ddot{\vec{r}}_i = \vec{F}_i^{\text{repulsion}} + \vec{F}_i^{\text{propulsion}} + \vec{F}_i^{\text{flocking}} + \vec{F}_i^{\text{noise}}$ was performed using the Newton-Stomer-Verlet algorithm with cell-based neighbor lists to expedite computation. Initializing the simulation with uniformly mixed populations, we found that they spontaneously phase separated with a dense region of active MASHers confined by passive MASHers. This occurs generally across parameter space, and appears to

be a product of the difference in preferred speeds between populations (see Supplemental Material [9]). For the parameter values studied here, this occurs in about $\sim 10^3 \times (r_0/v_0)$ time units and, once formed, remains stable for greater than $10^5 \times (r_0/v_0)$ time units.

We explored the model's phase space by varying $\alpha$ and $\sigma$ for the active MASHers over the intervals [0,1] and [0,3], respectively [Fig. 3(a)]. This led to $4.8 \times 10^5$ individual simulations sampled on $4.8 \times 10^3$ grid points. For each run, we measured the active MASHer rms angular momentum about their center of mass $x_{\text{c.m.}} = (L/2\pi)\arctan[\text{Im}(A)/\text{Re}(A)]$, where $L = 1.03\sqrt{\pi r_0^2 N}$ is the simulation box size, $A = \sum_{i=1}^{N_a} \exp(-2\pi i x_i/L)$, $N_a$ is the number of active MASHers, $x_i$ is the $x$ position of the $i$th MASHer, and a similar expression holds for $y_{\text{c.m.}}$. In the low-flocking, high-noise limit, we found the angular momentum was near zero, and upon closer inspection, discovered a gaslike region [Fig. 3(b)] where MASHers quantitatively reproduced the statistics found in experimentally observed mosh pits [Fig. 2(c)].

To interpret these results, we note that our model has three time scales: (i) the flocking time $\tau_{\text{flock}} = v_0/\alpha$, which can be found by dimensional analysis of Eq (3),

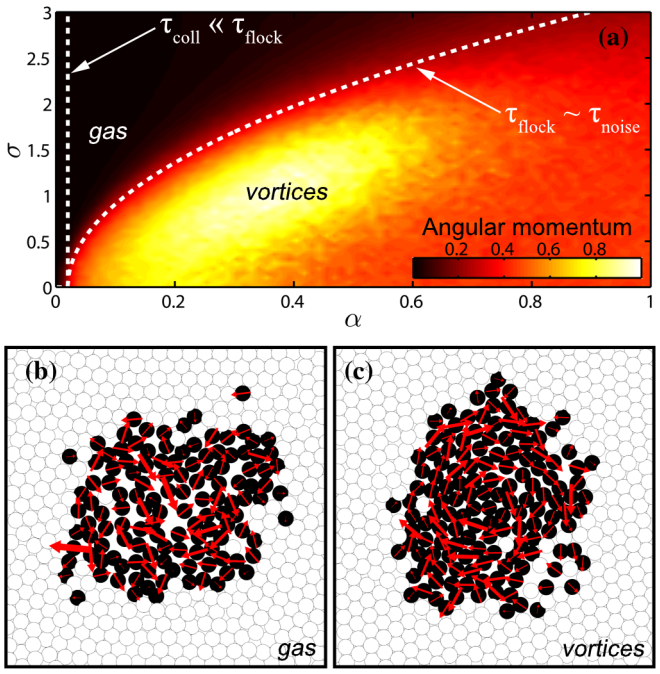


FIG. 3 (color online). (a) The rms angular momentum of active MASHers exhibits a disordered gaslike state in the high-noise low-flocking limit. The model also predicts an ordered vortexlike state in the low-noise moderate-flocking limit. Dashed white lines correspond to the bounds of the flocking-dominated regime. (b) Active MASHers (black) are confined by passive MASHers (white), and the velocity field (red arrows) resembles that found in actual mosh pits. (c) Active MASHers spontaneously self-organize into an ordered vortexlike state. (See movies 1 and 2 in the Supplemental Material [9].)

(ii) the noise time $\tau_{\text{noise}} = v_0^2/2\mu\sigma^2$, which can be found by calculating the amount of time required for noise to change the correlation function $\langle[v_i(\tau_{\text{noise}}) - v_i(0)]^2\rangle = 2\mu\sigma^2\tau_{\text{noise}}$ by an amount equal to the characteristic speed squared, and (iii) the collision time $\tau_{\text{coll}} = 1/(2r_0 v_0 \rho)$, which is the mean-free path $(2r_0\rho)^{-1}$ divided by the speed $v_0$. Both noise and collisions tend to randomize motion, whereas flocking tends to homogenize motion. Thus, when $\tau_{\text{noise}} \ll \tau_{\text{flock}}$, the statistical motion of the system is dominated by random forces. The boundary given by this condition occurs when $\tau_{\text{noise}} \sim \tau_{\text{flock}}$, or rather, $\sigma \sim \sqrt{v_0\alpha/\mu}$ [Fig. 3(a)]. Similarly, when the $\tau_{\text{coll}} \ll \tau_{\text{flock}}$, collisions cause disordered motion. This regime is bounded by $\alpha \ll 2r_0 v_0^2 \rho$, which is independent of $\sigma$, and for our choice of parameters is $\sim 1$; empirically, we find $\alpha \sim 10^{-2}$ in agreement with this condition. This demonstrates how a nonequilibrium system of moshers can have equilibrium characteristics: random motions induced by collisions or noise of self-propelled agents over a sufficient time reproduce the statistics of classical gases via the central limit theorem.

Conversely, when $\tau_{\text{flock}} \ll \tau_{\text{noise}}$ and $\tau_{\text{coll}}$, the flocking term dominates active MASHer motion. With sufficiently low noise, this limit of the model predicts a highly ordered vortexlike state [26,27] where MASHers again phase separate, but the confined active MASHers move with a large nonzero angular momentum [Fig. 3(c)]. Remarkably, this spontaneous phase separation and vortex formation is also observed at heavy metal concerts where they are conventionally called *circle pits* (Fig. 4; see Supplemental Material [9] for video metadata) [8]. In simulations, we found an even distribution between clockwise (CW) and counterclockwise (CCW) motion (when viewed from above) that switches directions at random intervals [28]. However, observations from concerts show 5% flow CW with the remaining 95% flowing CCW ($p < 0.001$). This asymmetry is independent of regional conventions in motor vehicle traffic, as video data were collected from a variety of countries including the United State of America, the United Kingdom, and Australia. Though the origin of this effect is unknown, we speculate it may be related to the dominant handedness or footedness found in humans, as it is known to bias turning behaviors [29].

The collective behavior described here has not been predicted on the basis of staged experiments with humans [30,31], making heavy metal concerts a unique model system for reliably, consistently, and ethically studying human collective motion. Currently, the most significant obstacle to further progress is the limited availability of publicly available high-quality video footage and a general reluctance among concert organizers to allow filming at their events. Nevertheless, further studies in this unique environment may enhance our understanding of collective motion in riots, protests, and panicked crowds, as it sheds light on what collective behaviors become possible when

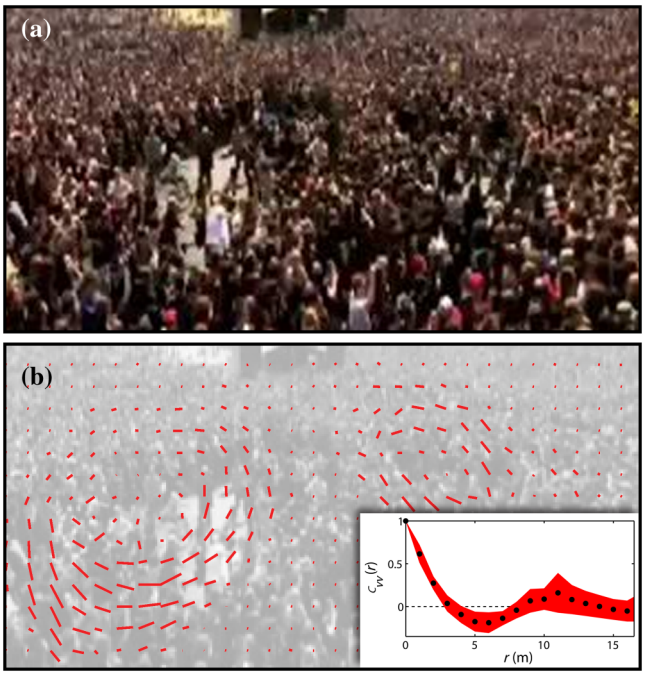


FIG. 4 (color online). The vortexlike state predicted in simulations is also observed at heavy metal concerts, where it is called a circle pit. (a) Single video frame illustrating two side-by-side circle pits [8]. (b) The same video image with overlaid velocity field. To facilitate comparisons with (a), this image is not corrected for perspective distortions. Inset shows the measured velocity-velocity correlation $c_{vv}$ as a function of distance $r$ (solid black circles, error estimates shown as red band). Note that $c_{vv}$ is maximally negative at $r \approx 6$ m, corresponding to the approximate diameter of the leftmost circle pit. Weak oscillations for $r > 6$ m are evident due to long-range correlations between the two circle pits.

traditional social rules are abandoned. Such studies may lead to new architectural safety design principles and crowd management strategies that limit the risk of injury at mass social gatherings [32]. For example, many heavy metal bands routinely announce during live performances, "If you see someone fall down in the mosh pit, pick them back up." This simple rule is known to reduce the risk of injury by trampling, and if employed in other extreme social gatherings, would be expected to have similar social benefits. Similarly, within the MASHer model, we found that by setting the preferred speed $v_0 = 0$, all mosh and circle pit behaviors ceased, suggesting an alternative approach to real-world crowd safety management.

Heavy metal concerts have the further advantage of exhibiting a rich variety of collective behaviors such as (i) the *wall of death* (moshers split into two groups separated by an open space and, when signaled, simultaneously run at the opposing group leading to a deliberate mass collision), (ii) *pogoing* (a locally correlated but globally decorrelated collective jumping), and (iii) propagating waves in jammed attendees [33]. In addition to these broadly defined types of collective motion, there are further variations that arise when concert organizers focus on specific musical subgenres that appeal to niche audiences. For example, *hardcore pits*, *ninja pits*, and *push pits* are all variants of the traditional mosh pit with their own unique characteristics that may not, when studied in detail, be well described by Eqs. (1)–(4). Thus, heavy metal concerts offer many new opportunities to study the collective behaviors arising from large groups of humans in extreme social conditions.

See Ref. [34] for information regarding source codes used herein.

The photo in Fig. 1 was taken and graciously provided by Ulrike Biets. J. L. S. and M. B. also thank D. Porter, L. Ristroph, J. Freund, J. Mergo, A. Holmes, A. Alemi, M. Flashman, K. Prabhakara, J. Wang, R. Lovelace, P. McEuen, S. Strogatz, the Cohen Lab, and the Sethna Group. Fieldwork was independently funded by J. L. S.

*JLS533@cornell.edu

[1] M. Moussaid, D. Helbing, and G. Theraulaz, Proc. Natl. Acad. Sci. U.S.A. **108**, 6884 (2011).
[2] D. Helbing, A. Johansson, and H. Z. Al-Abideen, Phys. Rev. E **75**, 046109 (2007).
[3] I. Farkas, D. Helbing, and T. Vicsek, Nature (London) **419**, 131 (2002).
[4] R. Walser, *Running with the Devil: Power, Gender, and Madness in Heavy Metal Music* (University Press of New England, Hanover, NH 1993).
[5] T. Janchar, C. Samaddar, and D. Milzman, Am. J. Emerg. Med. **18**, 62 (2000).
[6] A. B. Drake-Lee, J. R. Soc. Med. **85**, 617 (1992).
[7] M. S. C. Lim, M. E. Hellard, J. S. Hocking, and C. K. Aitken, Drug Alcohol Rev. **27**, 439 (2008).
[8] Over $10^5$ videos are available on YouTube.com illustrating mosh pits and circle pits. Some notable examples include http://youtu.be/5jKU7gdxncE, http://youtu.be/qkbOyg3NOiE, http://youtu.be/nOHY1YxX5iA, http://youtu.be/o7w7m4lb2ok, http://youtu.be/l6R7PiISaZw.
[9] See Supplemental Material at http://link.aps.org/supplemental/10.1103/PhysRevLett.110.228701 for video metadata, further details of PIV analysis, examples of phase separation, extended phase diagrams, example simulation videos, and a copy of the code used in simulations.
[10] C. Py, E. Langre, B. Moulia, and P. Hémon, Agr. Forest Meteorol. **130**, 223 (2005).
[11] J. K. Sveen and E. A. Cowen, in *PIV and Water Waves*, edited by J. Grue, P. L. F. Liu, and G. K. Pedersen (World Scientific, Singapore, 2003), Vol. 9, Chap. 1.
[12] N. Ashcroft, Sci. Am. **221**, No. 1, 72 (1969).
[13] L. F. Henderson, Nature (London) **229**, 381 (1971).
[14] L. Landau and E. Lifshitz, *Statistical Physics* (Elsevier, Oxford, 1980), 3rd ed., Chap. 3, Part 1.
[15] I. D. Couzin, J. Krause, R. James, G. Ruxton, and N. Franks, J. Theor. Biol. **218**, 1 (2002).
[16] A. Czirok, E. Ben-Jacob, I. Cohen, and T. Vicsek, Phys. Rev. E **54**, 1791 (1996).

[17] V. Schaller, C. Weber, C. Semmrich, E. Frey, and A. Bausch, Nature (London) **467**, 73 (2010).
[18] N. Leonard, T. Shen, B. Nabet, L. Scardovi, I. D. Couzin, and S. A. Levin, Proc. Natl. Acad. Sci. U.S.A. **109**, 227 (2012).
[19] D. Helbing and P. Molnar, Phys. Rev. E **51**, 4282 (1995).
[20] W. Bialek, A. Cavagna, I. Giardina, T. Mora, E. Silvestri, M. Viale, and A. M. Walczak, Proc. Natl. Acad. Sci. U.S.A. **109**, 4786 (2012).
[21] C. Reynolds, ACM SIGGRAPH Comput. Graph. **21**, 25 (1987).
[22] T. Vicsek and A. Zafeiris, Phys. Rep. **517**, 71 (2012).
[23] T. Vicsek, A. Czirok, E. Ben-Jacob, I. Cohen, and O. Shochet, Phys. Rev. Lett. **75**, 1226 (1995).
[24] S. K. You, D. H. Kwon, Y.-i. Park, S. M. Kim, M.-H. Chung, and C. K. Kim, J. Theor. Biol. **261**, 494 (2009).
[25] L. Landau and E. Lifshitz, *Theory of Elasticity* (Pergamon, New York, 1986), 3rd ed., Chap. 1.
[26] S. Bazazi, K. S. Pfennig, N. O. Handegard, and I. D. Couzin, Behav. Ecol. Sociobiol. **66**, 879 (2012).
[27] J. Toner, Y. Tu, and S. Ramaswamy, Ann. Phys. (Amsterdam) **318**, 170 (2005).
[28] H. Chen and Z. Hou, Phys. Rev. E **86**, 041122 (2012).
[29] C. Mohr, T. Landis, H. S. Bracha, and P. Brugger, Behav. Neurosci. **117**, 1448 (2003).
[30] M. Isobe, D. Helbing, and T. Nagatani, Phys. Rev. E **69**, 066132 (2004).
[31] M. Moussaid, D. Helbing, S. Garnier, A. Johansson, M. Combe, and G. Theraulaz, Proc. R. Soc. B **276**, 2755 (2009).
[32] D. Helbing, I. Farkas, and T. Vicsek, Nature (London) **407**, 487 (2000).
[33] L. E. Silbert, A. J. Liu, and S. R. Nagel, Phys. Rev. E **79**, 021308 (2009).
[34] Source code and a phase diagram generating PYTHON script are available under the M.I.T. license on github.com at https://github.com/mattbierbaum/moshpits. An interactive JAVASCRIPT version of the simulation is available at http://mattbierbaum.github.com/moshpits.js.